Assessment of the concomitant action of XBD173 and interferon β in a mouse model of multiple sclerosis using infrared marker bands

Krongkarn Sirinukunwattana, Christian Klein, Paul F A Clarke, Gilles Marcou, Laurence Meyer, Nicolas Collongues, Jérôme de Sèze, Petra Hellwig, Christine Patte-Mensah, Youssef El Khoury, et al.

Spectrochimica Acta Part A: Molecular and Biomolecular Spectroscopy 327 (2025) 125390

Contents lists available at ScienceDirect

Spectrochimica Acta Part A:
Molecular and Biomolecular Spectroscopy

journal homepage: www.journals.elsevier.com/spectrochimica-acta-part-a-molecular-and-biomolecular-spectroscopy

Assessment of the concomitant action of XBD173 and interferon β in a mouse model of multiple sclerosis using infrared marker bands

Krongkarn Sirinukunwattana [a], Christian Klein [b,c], Paul F.A. Clarke [d], Gilles Marcou [d], Laurence Meyer [b,c], Nicolas Collongues [b,c], Jérôme de Sèze [b,c], Petra Hellwig [a], Christine Patte-Mensah [b,c,1], Youssef El Khoury [a,*,1], Ayikoé-Guy Mensah-Nyagan [b,c,**,1]

[a] Laboratoire de bioélectrochimie et spectroscopie UMR 7140, Chimie de la matière complexe University of Strasbourg – CNRS 4, Rue Blaise Pascal F - 67081 Strasbourg, France
[b] Biopathologie de la Myéline, Neuroprotection et Stratégies Thérapeutiques, UMR_S1119, Faculty of Medicine, University of Strasbourg, 1, Rue Eugène Boeckel, 67000 Strasbourg, France
[c] Centre d'Investigation Clinique de Strasbourg (CIC), INSERM 1434, bâtiment CRBS, 1, Rue Eugène Boeckel, 67000 Strasbourg, France
[d] Laboratory of Chemoinformatics, UMR 7140 University of Strasbourg/CNRS, 4 Rue Blaise Pascal, 67000 Strasbourg, France

HIGHLIGHTS

- Infrared spectroscopy on RRMS mice sera detects significant alterations in protein and lipid signatures.
- RRMS mice treatment with low Interferon-β and XBD173 doses improves clinical scores and altered spectroscopic signature.
- XBD173 in combination with disease-modifying treatments appears as a good candidate for RRMS therapy.

GRAPHICAL ABSTRACT

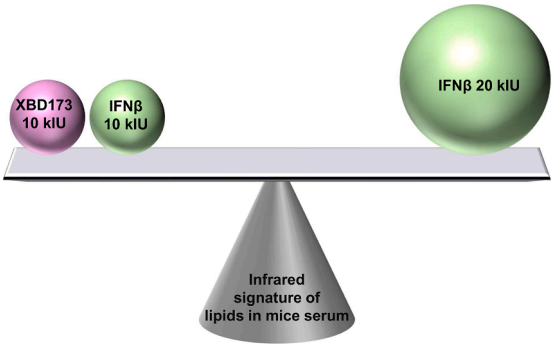

ARTICLE INFO

Keywords:
Multiple sclerosis
Infrared spectroscopy
Animal model
Interferon-β
XBD173

ABSTRACT

Disease modifying therapies including interferon-β (IFNβ) effectively counteract the inflammatory component in relapsing-remitting multiple sclerosis (RRMS) but this action, generally associated with severe side effects, does not prevent axonal/neuronal damages. Hence, axonal neuroprotection, which is pivotal for MS effective treatment, remains a difficult clinical challenge. Growing evidence suggested as promising candidate for neuroprotection, Emapunil (AC-5216) or XBD173, a ligand of the mitochondrial translocator protein highly expressed in glial cells and neurons. Indeed, elegant studies previously showed that low and well tolerated doses of XBD173 efficiently improved clinical symptoms and neuropathological markers in MS mice. Here we combined clinical scoring in vivo with Fourier transform infrared spectroscopy of sera samples to investigate the hypothesis that

* Corresponding author.
** Corresponding author at: Biopathologie de la Myéline, Neuroprotection et Stratégies Thérapeutiques, UMR_S1119, Faculty of Medicine, University of Strasbourg, 1, Rue Eugène Boeckel, 67000 Strasbourg, France.
E-mail addresses: elkhoury@unistra.fr (Y. El Khoury), gmensah@unistra.fr (A.-G. Mensah-Nyagan).
[1] Equal contributors.

https://doi.org/10.1016/j.saa.2024.125390
Received 22 July 2024; Received in revised form 10 October 2024; Accepted 2 November 2024
Available online 3 November 2024

the concomitant treatment of RRMS mice with low doses of IFNβ and XBD173 may increase their beneficial effects against MS symptoms and additionally decrease IFNβ-induced side effects. Our results show a significant alteration of the composition of serum protein and lipids in the spectra of the sera of RRMS mice. While the signature of proteins remains altered upon treatment, the signature of lipids is recovered comparatively well with 20 kIU IFNβ and upon concomitant treatment with a low dose of XBD173 (10 mg/kg) and IFNβ (10 kIU), but not with 10 kIU of IFNβ alone. The concomitant therapy with XBD173 (10 mg/kg) and IFNβ (10 kIU), devoid of side effects, exhibited at least equal or even better efficacy than IFNβ (20 kIU) treatment against RRMS symptoms.

1. Introduction

Multiple sclerosis (MS) is an auto-immune inflammatory demyelinating disease of the central nervous system affecting mainly female young adults below forty-four years old [1]. At disease onset, activated lymphocytes cross the blood–brain barrier (BBB) to the CNS causing demyelination and subsequent axonal damage as well as oligodendrocyte injury [2]. The MS course can be classified as relapsing-remitting (RRMS) or progressive (primary and secondary). RRMS, representing the most common form of MS with 80 % of prevalence in humans, is mimicked by the murine experimental autoimmune encephalomyelitis (EAE) model induced by the proteolipid protein (PLP) [3–5]. MS therapy relies mainly on disease-modifying treatments (DMT) such as immunomodulators and immunosuppressants, as well as neuroprotectors [6,7]. Among these DMTs, Interferon-β (IFNβ) which is a naturally-occurring cytokine was the first developed DMT and for a long time was the mainstream treatment of RRMS patients [8]. One of the most important effects of IFNβ is curbing inflammation (increase of anti-inflammatory and decrease of pro-inflammatory activities) [9]. Nowadays, more efficient and better tolerated DMT such as Natalizumab or anti-CD20 drugs are commonly used [10]. However, when disease progression occurred, no drug offers efficient neuroprotection apart from an anti-inflammatory effect, so that the definitive eradication of MS remains impossible. In addition, there are several side effects associated with MS medications including flu-like symptoms, chills, muscle and joint pain, liver dysfunctions, mood disorders [11,12]. Hence, the characterization of effective and safe MS drugs with no or little side effects remains a great challenge. In particular, there is a crucial need to target successfully pathophysiological mechanisms other than inflammation in order to develop effective neuroprotective drugs against MS. Therefore, several neuroprotective treatments are currently under investigation. In this perspective, recent pre-clinical research focused on the role of the translocator protein (TSPO) and its ligands [7]. Indeed, the 18 kDa mitochondrial membrane protein TSPO, highly expressed in glial cells and neurons [13–15] pivotally controls neuroprotective neurosteroid synthesis [16,17] and also exerts other essential functions such as the regulation of cell proliferation, apoptosis, immune response and bioenergetics [18,19]. Interestingly, previous investigations demonstrated that TSPO ligands induced significant improvement of MS mice symptoms [20–22]. In particular, the combination of solid clinical, behavioral, histopathological and biochemical/molecular methods revealed that low and well-tolerated doses (10 mg/kg) of TSPO ligand XBD173 (Emapunil) efficiently improved the clinical scores and neuropathological markers in RRMS (EAE-PLP) mice [21]. Therefore, we made the hypothesis that the concomitant injection of low doses of IFNβ and XBD173 may boost their beneficial actions against MS symptoms and additionally decrease IFNβ-related side effects. To check our hypothesis, we performed the present pilot study to determine the effects of separate and concomitant injections of selected doses of IFNβ and XBD173 on the clinical scores of controls and RRMS mice.

Fourier transform infrared (FTIR) spectroscopy is a sensitive, nondestructive, fast and cost-effective technique emerging for the analysis of body fluids, especially for disease diagnosis, prognosis and follow-up [23]. Typical mid infrared spectra of complex biological medium such as serum contain the signature of all the biological molecules present in the sample, including lipids, DNA and RNA, proteins, carbohydrates, etc. [23]. The characteristic contribution of (phospho) lipids [24] is known to dominate in the 3000–2825 cm^{-1} spectral range via the ν(CH) vibrational modes and around 1750 cm^{-1} via the ν(C═O) vibration of the ester of phospholipids. The proteins present in the serum have a specific signature. The most extensively studied protein band is the so-called amide I mode arising mainly from the ν(C═O) vibration of the protein backbone detectable between ~1700 and ~1600 cm^{-1}. This band is sensitive to the secondary structure of proteins with α-helices having a maximum at around 1654 cm^{-1}, random coils have a maximum at ~1640 cm^{-1} whereas beta-sheets can have several contributions at ~1685 and 1630 cm^{-1} [25]. Hence, amide I analysis [26,27] has been extensively used to follow secondary structure changes induced by certain diseases [28]. The data analysis of such infrared spectra, allowing sample classification based on pathophysiological parameters, may also contribute to the detection of small, yet significant differences in spectra reflecting the biochemical changes related to the disease progression and treatment responses. To get insights into the effects of XBD173 and IFNβ, we used FTIR spectroscopy of sera samples taken from the mice cohort to correlate the effect of treatments on the RRMS infrared marker bands. FTIR spectroscopy on blood biopsies are being used to develop reliable assays capable of reporting on MS disease progression and activity [29]. Immuno-based assays on serum proteins shows promising results for following and evaluating disease activity and progression [29–31]. We have previously shown that FTIR spectroscopy is sensitive towards small changes in the sera samples of patients, allowing to rapidly and accurately discriminate, RRMS sera samples and neuromyelitis optica spectrum disorders with the help of machine learning algorithm [32]. The sensitivity of the techniques allows detecting significant (often small) variations in the spectroscopic signature of patient serum samples induced by treatments.

Based upon these results, we decided to use the well-established RRMS mouse model, which successfully served in previous investigations of our group [21,22], to determine the efficacy of three therapeutic strategies aiming to treat RRMS clinical symptoms. Therefore, here we combined in vivo scoring of RRMS symptoms with FTIR spectroscopy of sera samples to compare the therapeutic potential of (i) a well-tolerated dosage of the neuroprotective compound XBD173 alone, (ii) interferon-β (IFNβ) therapy alone and (iii) a concomitant treatment with both XBD173 and IFNβ. The data analysis particularly focused on the spectroscopic signature of lipids and proteins, the two main components of myelin sheaths.

2. Methods

2.1. Animals

Nine-eleven-week-old SJL/jRj female mice were used in the present study. The mice were obtained from a commercial source (Janvier, Le Genest-St-Isle, France) and housed under standard laboratory conditions in a 12 h light/dark cycle with food and water ad libitum. Before starting the experiments, the animals were allowed a one-week acclimatization period after delivery in our animal house. Animal care and manipulations were conducted according to the European Community Council Directives (2010/63/UE) and under the supervision of authorized investigators. All experiments performed minimized the number of animals used and their suffering in accordance with the Alsace Department

of Veterinary Public Health Guide for the Care and Use of Laboratory Animals. A national project authorization was delivered by the French Ministry of Higher Education and Research and by CREMEAS a local ethical committee (Project authorization number 9374–201,605,111,128,746-v2). The experiments also followed the International Association for the Study of Pain ethical guidelines.

2.2. Production of RRMS (EAE-PLP) and control mice

EAE was induced in nine-eleven-week-old mice by subcutaneous injection of an emulsion containing 150 μg proteolipid protein (PLP139-151) peptide (Eurogentec, Liège, Belgium) emulsified 1:1 in Complete Freund's Adjuvant (CFA) to each hind flank (100 μL by flank). The CFA is prepared from Incomplete Freund's Adjuvant (IFA) (Santa Cruz Biotechnology, INC, Heidelberg, Germany) with *mycobacterium tuberculosis* (Difco Laboratories, Franklin Lakes, NJ) at 5 mg/mL. Then, the mice received 200 ng pertussis toxin (Enzo life sciences, Lausen, Swiss) in 200 μL sterile phosphate-buffered saline (PBS) intraperitoneally (i.p.) on day 0 and day 2 post-immunization (D0 and D2). Control mice were immunized without PLP139-151 according to a similar schedule. Clinical evaluation of symptoms was performed daily according to the standard EAE (RRMS) grading scale.

2.3. Drug treatment

XBD173 purchased from Sigma-Aldrich (Saint- Quentin-Fallavier, France) was dissolved in hydroxypropyl cellulose (HPC) 0.3 % (Alfa Aesar, Haverhill, Massachusetts, USA) before i.p. injection (200 μL) to mice at 10 mg/kg. IFNβ (TebuBio, France) was diluted in PBS before i.p. injection (100 μL) at 10 000 International Units (10 kIU) or 20 kIU.

The total cohort of 88 mice used for the present study was divided into 6 groups organized as follows: naive or healthy control mice (n = 7); RRMS (EAE-PLP) mice treated with IFNβ (10kIU) alone (n = 13); RRMS mice treated with IFNβ (20kIU) alone (n = 10); RRMS mice treated with XBD173 (10 mg/kg) alone (n = 20); RRMS mice concomitantly treated with XBD173 (10 mg/kg) + IFNβ (10kIU)(n = 15); RRMS mice concomitantly treated with HPC 0.3 % (vehicle for XBD173) + PBS (vehicle for IFNβ)(n = 23). Mice were treated every two days from D4 post immunization until sacrifice.

2.4. Sampling of serum, preparation conservation

The animals were sacrificed during the late remitting phase. They were deeply anesthetized with ketamine (200 mg/kg) / Rompun (20 mg/kg) (Centravet, France). Blood was removed, centrifuged at 1500 g at 4 °C for 30 min and the serum was stored at −80 °C until the beginning of FTIR spectroscopy experiments.

2.5. FTIR spectroscopy

The FTIR spectra of the sera samples were recorded with a Vertex 70 FTIR spectrometer from Bruker equipped with a Liquid-N2 cooled MCT detector. Each sample consisted of 2.5 μL of serum left to form a film on the surface of a diamond ATR crystal. For each sample, 10 spectra of 64 scans are averaged. The spectral resolution is 4 cm^{-1}. For each spectrum, a baseline correction and Min-max normalization are performed before derivation. For each class of samples (i.e. naïve, vehicle, etc.) an average derivative is calculated, and the standard deviation is calculated for each data point. Afterwards, the area under each signal of interest is calculated and plotted for the six classes of samples. The plots allow following the changes in the sera samples according to the disease status as well as following the effect of treatment.

2.6. Statistical analysis of the clinical scores

All data represent the mean ± SEM. Statistical differences were assessed by Kruskal-Wallis One-Way analysis of variance (ANOVA) followed by Dunn's multiple comparisons test. Statistical analysis was performed with GraphPad-Prism software (GraphPad-Prism, San Diego, CA, USA). A p-value ≤0.05 was considered significant (versus naïve * $p \leq 0.05$, ** $p \leq 0.01$, *** $p \leq 0.001$, **** $p \leq 0.0001$ or versus vehicle # $p \leq 0.05$, ## $p \leq 0.01$, ### $p \leq 0.001$, #### $p \leq 0.0001$).

3. Results and discussion

3.1. Clinical scores and drug effects on disease progression

Treatment of RRMS mice with XBD173 was compared to IFNβ alone and concomitant administration of XBD173 and IFNβ. Table 1 shows the mice cohorts and their average clinical scores at the disease peak (D14-D16) and at the late remitting phase (D35-D37) which corresponded to the moment of sacrifice and blood sample collections. The individual clinical scores of each mouse and statistical analysis with multiple comparison tests are available in Tables S1, S2 and S3 of the Supplementary data.

The results reveal a beneficial effect (clinical score decrease) of the treatments with XBD173 (10 mg/kg) alone, IFNβ (20 kIU) alone and concomitant [IFNβ (10 kIU) + XBD173 (10 mg/kg)] that occurred as a strong tendency since D14-D16 (disease peak) and has become clearly significant statistically at D35-D37 (sacrifice and blood sample collection). The treatment with IFNβ (10 kIU) alone was ineffective. But interestingly, we observed that the co-administration of [IFNβ (10 kIU) + XBD173 (10 mg/kg)] was strongly effective in preventing/protecting against the disease progression since the average clinical score detected under this concomitant treatment (0.80 ± 0.26) was not statistically different from the value of the naïve/healthy control mice (0.00). Taken together, our clinical results show that the co-administration of low and

Table 1
Cohorts of mice included in this study along with their average clinical scores (mean ± SEM) at the peak and at the moment of sacrifice and blood samples collection. The standard grading scale ranges from 0 to 10 where a score of 0 indicates the absence of clinical signs. Higher clinical scores reflect disease worsening with a maximal score of 10 indicating death. A p-value ≤ 0.05 was considered significant (versus naïve * $p \leq 0.05$, ** $p \leq 0.01$, *** $p \leq 0.001$, **** $p \leq 0.0001$ or versus vehicle # $p \leq 0.05$, ## $p \leq 0.01$, ### $p \leq 0.001$, #### $p \leq 0.0001$). The individual clinical scores of each mouse are listed in supporting Table S1 and the results of multiple parameter statistical comparisons are presented in Tables S2 and S3.

Cohort		Total number of mice	At peak (D14-J16)		At the moment of sacrifice (D35-D37)	
			Average clinical score ± SEM	p	Average clinical score ± SEM	p
Naïve (healthy controls)		7	0.00	# # # #	0.00	# # # #
Vehicle (untreated RRMS)		23	3.35 ± 0.27	* * * *	2.93 ± 0.33	* * * *
Treated RRMS	IFNβ 10kIU	13	3.23 ± 0.43	* * * *	2.58 ± 0.62	* * *
	IFNβ 20kIU	10	2.50 ± 0.48	* *	1.60 ± 0.54	* #
	10 mg/kg XBD173	20	2.70 ± 0.23	* * *	1.30 ± 0.36	* # # #
	10 mg/kg XBD173 + IFNβ 10kIU	15	2.47 ± 0.24	* *	0.80 ± 0.26	# # #

well tolerated dose of XBD173 (10 mg/kg) with an inactive/low dose of IFNβ (10 kIU) induced an additive and/or synergistic increase of the beneficial effect against RRMS symptoms that appears better than the protective action exerted by the elevated dose of IFNβ (20 KIU) which is effective but generally evokes various side effects when injected alone.

3.2. FTIR spectroscopy on the sera samples

To investigate the effect of treatment, we collected sera samples and recorded their FTIR spectra to check for vibrational markers of disease activity and how the treatments affect these markers. Fig. 1 shows the ensemble of the recorded spectra. The data are very similar to data we recorded on sera taken from human subjects [32,33], The 3600–2800 cm^{-1} spectral range is dominated by signals arising from the ν(N−H) vibration, i.e. amide-A of proteins and ν(C−H) vibrations of lipids. Below 1800 cm^{-1} signals from phospholipids, proteins, nucleic acids and carbohydrates are present. The complete assignments of the signals are shown in Table S4.

The comparison of the FTIR spectra of healthy vs. RRMS mice sera samples shows that the amide I band arising from proteins is significantly affected by the disease. Indeed, the FTIR spectrum of serum of RRMS mice shows a significant loss of the absorption of α-helices in RRMS mice and none of the treatments helps significantly recovering this loss (Fig. 2). In addition, a higher β-sheets contribution is observed compared to the sera of healthy mice. Only IFNβ treatment leads to a decrease of the β-sheets contribution. The decrease is proportional to the administrated dose of the IFNβ, yet 20 kIU of IFNβ do not bring back the β-sheets contribution to baseline values.

Thus, IFNβ curbs the increase of the β-sheet/α-helix ratio in the amide I band. This ratio is a vibrational marker of inflammation. This is in line with results published by other groups on RRMS patients [34] where the authors assigned the β-sheets to amyloid-β peptides and to a possible secondary change of myelin proteins. In our previous studies, we have also observed that there in an increase in the infrared absorption of β-sheets in the progressive form of MS but not in the relapsing-remitting form [32,33].

In addition, the absorption of the ν(C═O) vibration of the ester of phospholipids centered at 1743 cm^{-1} becomes lower in intensity in spectra of the sera of RRMS (Fig. 2). This was previously shown for sera samples of RRMS patients (Phosphatidylcholine, Lysol Phosphatidylcholine and sphingomyelin) [35], Treatment with either IFNβ or XBD173 allows to partially recover the contribution of the phospholipids and there is no significant difference between the treatment with 20 kIU IFNβ and the other treatments.

The higher wavenumber range of the infrared spectrum of serum is characterized by the absorptions from $\nu_{as/s}$(C−H) vibrations of CH_2 and CH_3 of lipids. The second derivatives of the average spectra of the different groups of mice sera (Fig. 3A) and the corresponding areas under curve (Fig. 3B) show that the disease decreases the contribution of lipids. The 10 kIU dose of IFNβ is not capable of restoring the loss of the lipids' signals. The effect of the treatment with 10 mg/kg XBD173 alone is comparable to the one of 10 kIU IFNβ. Yet, treatment with either 20 kIU IFNβ or the mixture of 10 kIU IFNβ + 10 mg/kg XBD173 yield a restored signal of the lipids in the RRMS diseased mice.

Below 1300 cm^{-1}, signals arising from DNA and RNA as well as carbohydrates can be observed. The disease leads to an imbalance in the signature of these molecules. For instance, the signals arising from the $\nu_{as}(PO_2^-)$ vibration of DNA at 1239 cm^{-1} becomes more intense in the spectrum of serum of RRMS mice compared to the control (Fig. 4) whereas the signals arising from the υ(C–O) vibration of carbohydrates at 1170 cm^{-1} and RNA at 1123 cm^{-1} lose intensity. The examination of the areas of these signals in the different groups of mice shows that only the 20 kIU IFNβ dose helps countering the effect of the disease.

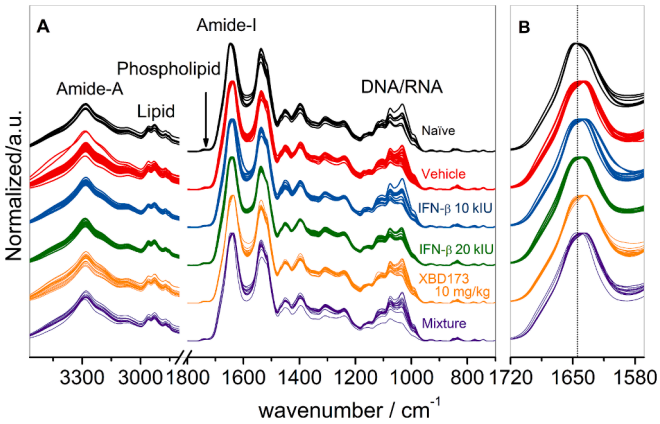

Fig. 1. A) FTIR spectra of all the sera samples recorded between 3600 and 700 cm^{-1}. Naïve spectra are shown in black, Vehicle's in red, IFNβ 10 kIU's in blue, IFNβ 20 kIU's in green, XBD's in orange and the mixture of XBD + IFNβ's in violet. B) Enlarged view of the amide I bands. The vertical line is placed at the center of the amide I band of naïve's spectra. It serves as a guide to the eye to better see the shifts of the amide I maxima of the different groups of spectra relative to the one of naive.

4. Conclusions

The RRMS in mice model has a substantial effect on the infrared spectrum of serum. Indeed, a significantly larger contribution of β-sheets is observed for RRMS mice compared to the naïve ones. Similarly, a significant loss of absorption arising from lipids is detected in RRMS mice. The various treatments administered to the RRMS mice reduce the clinical score. Yet only the 20 kIU dose of IFNβ has a significant role in improving β-sheet/α-helix ratio in the amide I band. On the other hand, while XBD173 alone leads to lower clinical scores, it does not seem to have a significant effect on the spectra of sera of RRMS. However, the mixture of a lower dose of IFN (10 kIU IFNβ) with 10 mg/kg of XBD173 yields a comparable effect to the treatment with 20 kIU IFNβ concerning the signature of lipids in the serum.

The significant increase of the β-sheet character of the proteins in the serum does not seem to be correlate with the clinical scores' evolution upon treatment since the improvement of the clinical scores' is observed for either treatment, whereas only IFNβ curbs the contribution of the β-sheet type proteins. The alteration of the composition of serum lipids is however in line with the evolution of the clinical scores. Finally, the combination of 10 mg/kg XBD173 with a lower dose of IFNβ has a synergetic effect yielding lower clinical scores in RRMS mice. Thus, XBD173 is a good candidate to be tested in RRMS mice model in combination with the current DMTs used in the clinic.

Author contributions

C. Patte-Mensah, C. Klein, L. Meyer: Production of EAE/RRMS and control mice, clinical scoring, blood sample collection and data analysis. AG. Mensah-Nyagan and C. Patte-Mensah: Study conception and design, supervision, analysis and interpretation of data, manuscript writing and editing. N. Collongues and J. de Sèze: Critical reading and editing. K. Sirinukunwattana Collected FTIR data and performed data analysis. P. F. A. Clarke and G. Marcou contributed to the data analysis. P. Hellwig contributed to the data analysis, reading and editing the manuscript. Y. El Khoury supervised the spectroscopy experiments, performed data analysis and drafted the manuscript. All authors read and approved the submitted manuscript.

Declaration of competing interest

The authors declare that they have no known competing financial

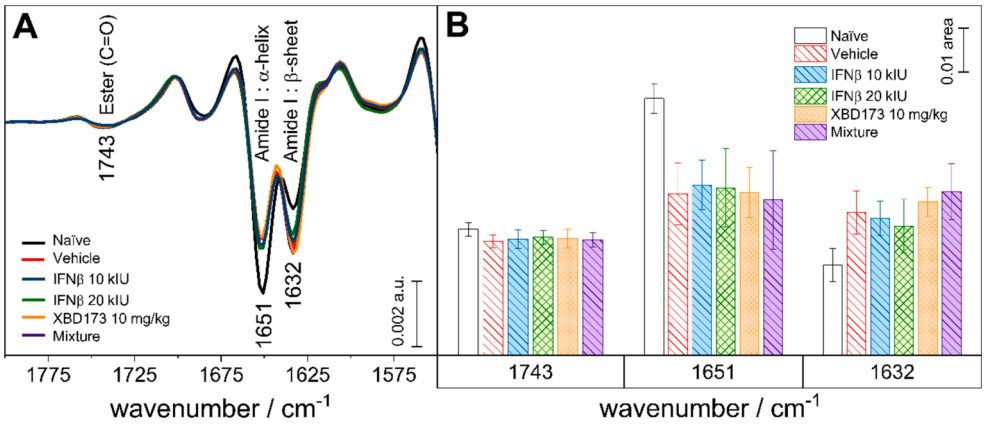

Fig. 2. A) Second derivatives of the average spectra of each group of mice in the 1800–1500 cm^{-1} spectral range. B) Average areas under curve for each of the signals centered at 1743, 1651 and 1632 cm^{-1}.

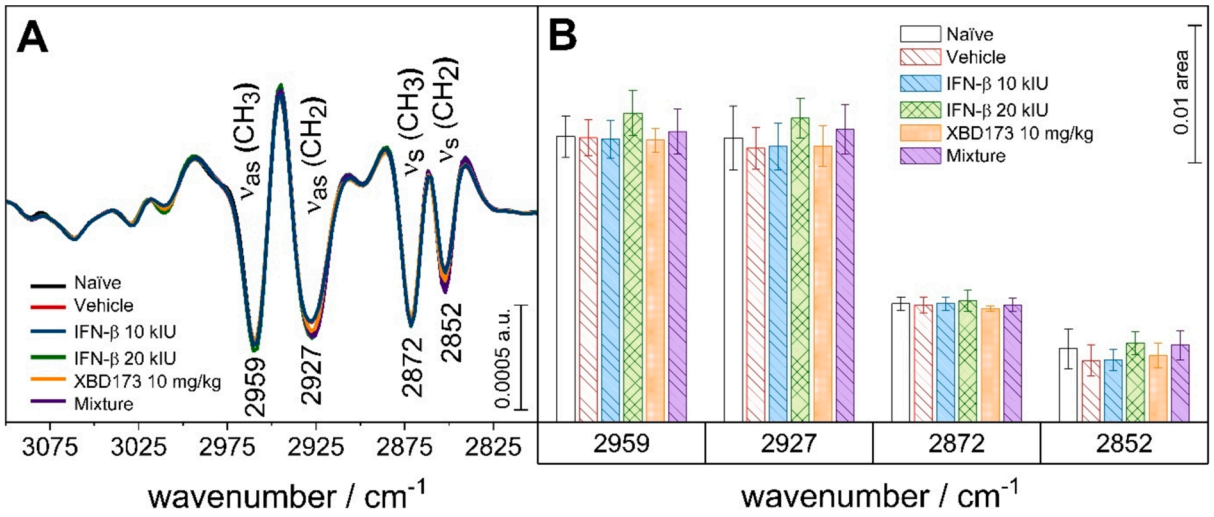

Fig. 3. A) Second derivatives of the average spectra of each group of mice in the 3100–2800 cm^{-1} spectral range. B) Average areas under curve for each of the signals centered at 2959, 2927, 2872 and 2852 cm^{-1}.

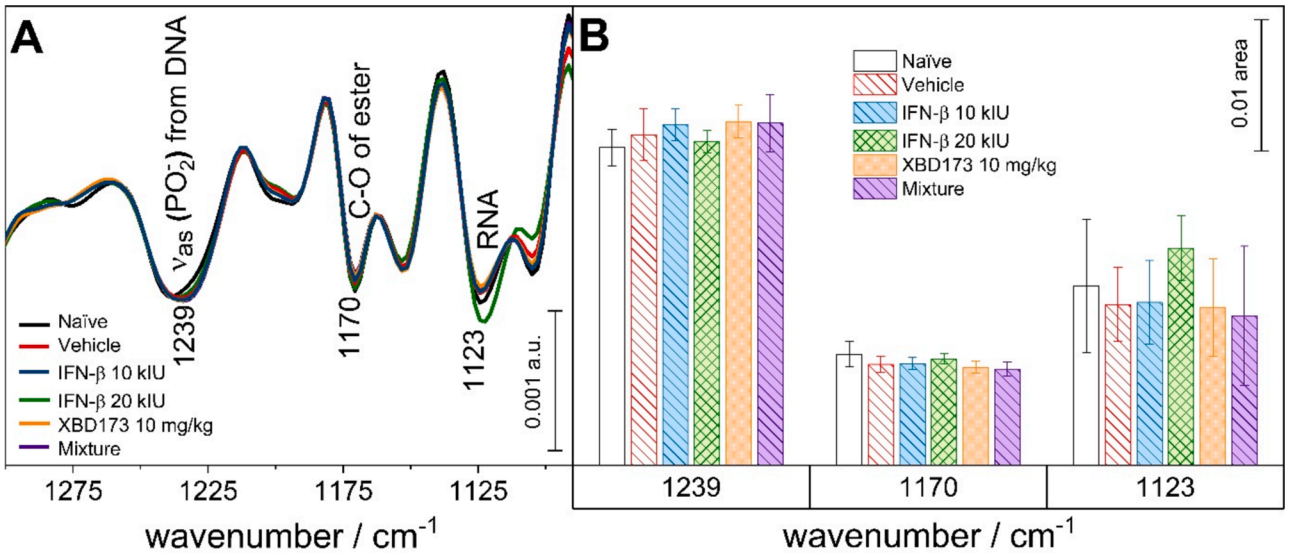

Fig. 4. A) Second derivatives of the average spectra of each group of mice in the 1300–1180 cm^{-1} spectral range. B) Average areas under curve for each of the signals centered at 1239, 1170 and 1123 cm^{-1}.

interests or personal relationships that could have appeared to influence the work reported in this paper.

Acknowledgements

This work was supported by the Royal Thai government, P. H. thanks the Interdisciplinary Thematic Institute SysChem for funding via the IdEx Unistra (ANR-10-IDEX-0002) within the Programme Investissement d'Avenir as well as the Institut Universitaire de France. We thank also the Institut National de la Santé et de la Recherche Médicale (INSERM, France, grant #U1119) and Université of Strasbourg (France, grant #UMR_S 1119).

Appendix A. Supplementary data

Supplementary data to this article can be found online at https://doi.org/10.1016/j.saa.2024.125390.

Data availability

Data will be made available on request.

References

[1] C. Walton, R. King, L. Rechtman, W. Kaye, E. Leray, R.A. Marrie, N. Robertson, N. La Rocca, B. Uitdehaag, I. van der Mei, M. Wallin, A. Helme, C. Angood Napier, N. Rijke, P. Baneke, Rising prevalence of multiple sclerosis worldwide: Insights from the Atlas of MS, third edition, Mult. Scler., 26 (2020) 1816-1821.
[2] C.A. Dendrou, L. Fugger, M.A. Friese, Immunopathology of multiple sclerosis, Nat. Rev. Immunol. 15 (2015) 545–558.
[3] M. Kipp, S. Nyamoya, T. Hochstrasser, S. Amor, Multiple sclerosis animal models: a clinical and histopathological perspective, Brain Pathol. 27 (2017) 123–137.
[4] A.P. Robinson, C.T. Harp, A. Noronha, S.D. Miller, The experimental autoimmune encephalomyelitis (EAE) model of MS: utility for understanding disease pathophysiology and treatment, Handb. Clin. Neurol. 122 (2014) 173–189.
[5] C.S. Constantinescu, N. Farooqi, K. O'Brien, B. Gran, Experimental autoimmune encephalomyelitis (EAE) as a model for multiple sclerosis (MS), Br. J. Pharmacol. 164 (2011) 1079–1106.
[6] J.H. Yang, T. Rempe, N. Whitmire, A. Dunn-Pirio, J.S. Graves, Therapeutic advances in multiple sclerosis, Front. Neurol. 13 (2022) 824926.
[7] N. Collongues, G. Becker, V. Jolivel, E. Ayme-Dietrich, J. de Seze, F. Biname, C. Patte-Mensah, L. Monassier, A.G. Mensah-Nyagan, A narrative review on axonal neuroprotection in multiple sclerosis, Neurol. Ther. 11 (2022) 981–1042.
[8] M. Filipi, S. Jack, Interferons in the treatment of multiple sclerosis: a clinical efficacy, safety, and tolerability update, Int. J. MS Care 22 (2020) 165–172.
[9] B.C. Kieseier, The mechanism of action of interferon-beta in relapsing multiple sclerosis, CNS Drugs 25 (2011) 491–502.
[10] H. Butzkueven, L. Kappos, H. Wiendl, M. Trojano, T. Spelman, I. Chang, R. Kasliwal, S. Jaitly, N. Campbell, P.R. Ho, S. Licata, I. Tysabri, Observational Program, Long-term safety and effectiveness of natalizumab treatment in clinical practice: 10 years of real-world data from the Tysabri Observational Program (TOP), J. Neurol. Neurosurg. Psychiatry 91 (2020) 660–668.
[11] C. Eckstein, M.T. Bhatti, Currently approved and emerging oral therapies in multiple sclerosis: An update for the ophthalmologist, Surv. Ophthalmol. 61 (2016) 318–332.
[12] C. McNamara, G. Sugrue, B. Murray, P.J. MacMahon, Current and emerging therapies in multiple sclerosis: implications for the radiologist, Part 1-Mechanisms, efficacy, and safety, Am. J. Neuroradiol. 38 (2017) 1664–1671.
[13] V. Papadopoulos, M. Baraldi, T.R. Guilarte, T.B. Knudsen, J.J. Lacapère, P. Lindemann, M.D. Norenberg, D. Nutt, A. Weizman, M.R. Zhang, M. Gavish, Translocator protein (18kDa): new nomenclature for the peripheral-type benzodiazepine receptor based on its structure and molecular function, Trends Pharmacol. Sci. 27 (2006) 402–409.
[14] Y. Lee, Y. Park, H. Nam, J.W. Lee, S.W. Yu, Translocator protein (TSPO): the new story of the old protein in neuroinflammation, BMB Rep. 53 (2020) 20–27.
[15] T. Notter, J.M. Coughlin, A. Sawa, U. Meyer, Reconceptualization of translocator protein as a biomarker of neuroinflammation in psychiatry, Mol. Psychiatry 23 (2018) 36–47.
[16] A.G. Mensah-Nyagan, J.L. Do-Rego, D. Beaujean, V. Luu-The, G. Pelletier, H. Vaudry, Neurosteroids: expression of steroidogenic enzymes and regulation of steroid biosynthesis in the central nervous system, Pharmacol. Rev. 51 (1999) 63–81.
[17] R. Rupprecht, V. Papadopoulos, G. Rammes, T.C. Baghai, J. Fan, N. Akula, G. Groyer, D. Adams, M. Schumacher, Translocator protein (18 kDa) (TSPO) as a therapeutic target for neurological and psychiatric disorders, Nat. Rev. Drug Discov. 9 (2010) 971–988.
[18] C.R. Hatty, R.B. Banati, Protein-ligand and membrane-ligand interactions in pharmacology: the case of the translocator protein (TSPO), Pharmacol. Res. 100 (2015) 58–63.
[19] C. Betlazar, R.J. Middleton, R. Banati, G.J. Liu, The translocator protein (TSPO) in mitochondrial bioenergetics and immune processes, Cells 9 (2020).
[20] D.J. Daugherty, V. Selvaraj, O.V. Chechneva, X.B. Liu, D.E. Pleasure, W. Deng, A TSPO ligand is protective in a mouse model of multiple sclerosis, EMBO Mol. Med. 5 (2013) 891–903.
[21] G. Leva, C. Klein, J. Benyounes, F. Halle, F. Bihel, N. Collongues, J. De Seze, A. G. Mensah-Nyagan, C. Patte-Mensah, The translocator protein ligand XBD173 improves clinical symptoms and neuropathological markers in the SJL/J mouse model of multiple sclerosis, Biochim. Biophys. Acta Mol. Basis Dis. 2017 (1863) 3016–3027.
[22] C. Tremolanti, C. Cavallini, L. Meyer, C. Klein, E. Da Pozzo, B. Costa, L. Germelli, S. Taliani, C. Patte-Mensah, A.G. Mensah-Nyagan, Translocator protein ligand PIGA1138 reduces disease symptoms and severity in experimental autoimmune encephalomyelitis model of primary progressive multiple sclerosis, Mol. Neurobiol. 59 (2022) 1744–1765.
[23] A.L. Mitchell, K.B. Gajjar, G. Theophilou, F.L. Martin, P.L. Martin-Hirsch, Vibrational spectroscopy of biofluids for disease screening or diagnosis: translation from the laboratory to a clinical setting, J. Biophotonics 7 (2014) 153–165.
[24] X. Chen, Z.A. Al-Mualem, C.R. Baiz, Lipid landscapes: vibrational spectroscopy for decoding membrane complexity, Annu. Rev. Phys. Chem. 75 (2024) 283–305.
[25] A. Barth, C. Zscherp, What vibrations tell us about proteins, Q. Rev. Biophys. 35 (2002) 369–430.
[26] J. Kong, S. Yu, Fourier transform infrared spectroscopic analysis of protein secondary structures, Acta Biochim. Biophys. Sin. 39 (2007) 549–559.
[27] S. Yang, Q. Zhang, H. Yang, H. Shi, A. Dong, L. Wang, S. Yu, Progress in infrared spectroscopy as an efficient tool for predicting protein secondary structure, Int. J. Biol. Macromol. 206 (2022) 175–187.
[28] L.M. Miller, M.W. Bourassa, R.J. Smith, FTIR spectroscopic imaging of protein aggregation in living cells, Biochim. Biophys. Acta Biomembr. 2013 (1828) 2339–2346.
[29] T. Chitnis, J. Foley, C. Ionete, N.K. El Ayoubi, S. Saxena, P. Gaitan-Walsh, H. Lokhande, A. Paul, F. Saleh, H. Weiner, F. Qureshi, M.J. Becich, F.R. da Costa, V. M. Gehman, F. Zhang, A. Keshavan, K. Jalaleddini, A. Ghoreyshi, S.J. Khoury, Clinical validation of a multi-protein, serum-based assay for disease activity assessments in multiple sclerosis, Clin. Immunol. 253 (2023) 109688.
[30] C. Barro, B.C. Healy, S. Saxena, B.I. Glanz, A. Paul, M. Polgar-Turcsanyi, C. R. Guttmann, R. Bakshi, H.L. Weiner, T. Chitnis, Serum NfL but not GFAP predicts cognitive decline in active progressive multiple sclerosis patients, Mult. Scler. 29 (2023) 206–211.
[31] A.S. Malinick, D.D. Stuart, A.S. Lambert, Q. Cheng, Surface plasmon resonance imaging (SPRi) in combination with machine learning for microarray analysis of multiple sclerosis biomarkers in whole serum, Biosens. Bioelectron. 10 (2022) 100127.
[32] Y. El Khoury, M. Gebelin, J. de Sèze, C. Patte-Mensah, G. Marcou, A. Varnek, A. G. Mensah-Nyagan, P. Hellwig, N. Collongues, Rapid discrimination of neuromyelitis optica spectrum disorder and multiple sclerosis using machine learning on infrared spectra of sera, Int. J. Mol. Sci. 23 (2022).
[33] Y. El Khoury, N. Collongues, J. De Sèze, V. Gulsari, C. Patte-Mensah, G. Marcou, A. Varnek, A.G. Mensah-Nyagan, P. Hellwig, Serum-based differentiation between multiple sclerosis and amyotrophic lateral sclerosis by Random Forest classification of FTIR spectra, Analyst 144 (2019) 4647–4652.
[34] M. Kolodziej, K. Chrabaszcz, E. Pieta, N. Piergies, J. Rudnicka-Czerwiec, H. Bartosik-Psujek, C. Paluszkiewicz, M. Cholewa, W.M. Kwiatek, Spectral signature of multiple sclerosis. Preliminary studies of blood fraction by ATR FTIR technique, Biochem. Biophys. Res. Commun. 593 (2022) 40–45.
[35] H.B. Ferreira, T. Melo, A. Monteiro, A. Paiva, P. Domingues, M.R. Domingues, Serum phospholipidomics reveals altered lipid profile and promising biomarkers in multiple sclerosis, Arch. Biochem. Biophys. 697 (2021) 108672.